SIAM J. NUMER. ANAL.
Vol. 43, No. 2, pp. 750–766

POLYNOMIALS AND POTENTIAL THEORY FOR GAUSSIAN RADIAL BASIS FUNCTION INTERPOLATION*

RODRIGO B. PLATTE† AND TOBIN A. DRISCOLL†

Abstract. We explore a connection between Gaussian radial basis functions and polynomials. Using standard tools of potential theory, we find that these radial functions are susceptible to the Runge phenomenon, not only in the limit of increasingly flat functions, but also in the finite shape parameter case. We show that there exist interpolation node distributions that prevent such phenomena and allow stable approximations. Using polynomials also provides an explicit interpolation formula that avoids the difficulties of inverting interpolation matrices, while not imposing restrictions on the shape parameter or number of points.

Key words. Gaussian radial basis functions, RBF, potential theory, Runge phenomenon, convergence, stability

AMS subject classifications. 65D05, 41A30

DOI. 10.1137/040610143

1. Introduction.

Radial basis functions (RBFs) have been popular for some time in high-dimensional approximation [3] and are increasingly being used in the numerical solution of partial differential equations [7, 14, 17, 20]. Given a set of *centers* $\xi_0, \ldots, \xi_N$ in R^d, an RBF approximation takes the form

$$F(x) = \sum_{k=0}^{N} \lambda_k \, \phi\big(\|x - \xi_k\|\big), \tag{1.1}$$

where $\|\cdot\|$ denotes the Euclidean distance between two points and $\phi(r)$ is a function defined for $r \geq 0$. The coefficients $\lambda_0, \ldots, \lambda_N$ may be chosen by interpolation or other conditions at a set of *nodes* that typically coincide with the centers. In this article, however, we give special attention to the case in which the locations of centers and nodes differ. Moreover, we shall consider equally spaced centers in most parts of this exposition.

Common choices for ϕ fall into two main categories:

- infinitely smooth and containing a free parameter, such as multiquadrics ($\phi(r) = \sqrt{r^2 + c^2}$) and Gaussians ($\phi(r) = e^{-(r/c)^2}$);
- piecewise smooth and parameter-free, such as cubics ($\phi(r) = r^3$) and thin plate splines ($\phi(r) = r^2 \ln r$).

Convergence analysis of RBF interpolation has been carried out by several researchers—see, e.g., [18, 19, 25]. For smooth ϕ, spectral convergence has been proved for functions belonging to a certain reproducing kernel Hilbert space $\mathcal{F}_\phi$ [19]. This space, however, is rather small since the Fourier transform of functions in $\mathcal{F}_\phi$ must decay very quickly or have compact support [25]. More recently, in [26] Yoon obtained spectral orders on Sobolev spaces, and in [11] error analysis was performed by considering the simplified case of equispaced periodic data. In this article, we use standard

*Received by the editors June 17, 2004; accepted for publication (in revised form) November 18, 2004; published electronically August 31, 2005. This research was supported by National Science Foundation grant DMS-0104229.

http://www.siam.org/journals/sinum/43-2/61014.html

†Department of Mathematical Sciences, University of Delaware, Newark, DE 19716 (platte@math.udel.edu, driscoll@math.udel.edu).

tools of polynomial interpolation and potential theory to study several properties of Gaussian RBF (GRBF) interpolation in one dimension, including convergence and stability.

As is well known in polynomial interpolation, a proper choice of interpolation nodes is essential for good approximations. It is also known that, for fixed N in the limit $c \to \infty$, RBF interpolation is equivalent to polynomial interpolation on the same nodes [6]; hence, the classical Runge phenomenon, and its remedy through node spacing, applies. For practical implementations it is well appreciated that node clustering near the boundaries is helpful [10, 20], but to our knowledge there has been no clear statement about the Runge phenomenon or asymptotically stable interpolation nodes for finite-parameter RBFs. The question has perhaps been obscured somewhat by the fact that the straightforward approach to computing the λ_k is itself numerically ill-conditioned when the underlying approximations are accurate [22].

In this paper we explore the fact that GRBFs with equally spaced centers are related to polynomials through a simple change of variable. Using this connection, in section 2 we demonstrate a Runge phenomenon using GRBFs on equispaced and classical Chebyshev nodes, and we compute asymptotically optimal node densities using potential theory. Numerical calculations suggest that these node densities give Lebesgue constants that grow at logarithmic rates, allowing stable approximations. In section 3 we explore the algorithmic implications of the connections we have made and derive a barycentric interpolation formula that circumvents the difficulty of inverting a poorly conditioned matrix, so approximations can be carried out to machine precision without restrictions on the values of the shape parameter c and number of centers N. Finally, section 4 contains observations on multiquadrics and other possible extensions of the methods presented.

2. Gaussian RBFs as polynomials. In (1.1) we now choose $d = 1$, Gaussian shape functions, and centers $\xi_k = -1 + 2k/N = -1 + kh$, $k = 0, \ldots, N$. Hence the GRBF approximation is

$$F(x) = \sum_{k=0}^{N} \lambda_k e^{-(x+1-kh)^2/c^2} = e^{-(x+1)^2/c^2} \sum_{k=0}^{N} \lambda_k e^{(2kh-k^2h^2)/c^2} e^{2kxh/c^2}. \tag{2.1}$$

Making the definition $\beta = 2h/c^2 = 4/(Nc^2)$ and using the transformation

$$s = e^{\beta x}, \quad s \in [e^{-\beta}, e^{\beta}],$$

we find that

$$G(s) = F\left(\frac{\log(s)}{\beta}\right) = e^{-\frac{N}{4\beta}(\log s+\beta)^2} \sum_{k=0}^{N} \tilde{\lambda}_k s^k = \psi_\beta^N(s) \sum_{k=0}^{N} \tilde{\lambda}_k s^k, \tag{2.2}$$

where the $\tilde{\lambda}_k$ are independent of s. In this section we regard β as a fixed parameter of the GRBF method. In the literature this is sometimes called the stationary case [2].

From (2.2) it is clear that G/ψ_β^N is a polynomial of degree no greater than N. If F is chosen by interpolation to a given f at $N+1$ nodes, then we can apply standard potential theory to find necessary convergence conditions on the singularities of f in the complex plane $z = x + iy$.

LEMMA 2.1. *Suppose that f is analytic in a closed simply connected region R that lies inside the strip $-\pi/(2\beta) < \mathrm{Im}(z) < \pi/(2\beta)$ and that C is a simple, closed,*

rectifiable curve that lies in R and contains the interpolation points $x_0, x_1, \ldots, x_N$. Then the remainder of the GRBF interpolation for f at x can be represented as the contour integral

$$f(x) - F(x) = \frac{\beta \eta_N(x)}{2\pi i} \int_C \frac{f(z) e^{\beta z}}{\eta_N(z)(e^{\beta z} - e^{\beta x})} dz,$$

where $\eta_N(x) = e^{-\frac{N\beta}{4}(x+1)^2} \prod_{k=0}^{N} (e^{\beta x} - e^{\beta x_k})$.

Proof. Consider the conformal map $w = e^{\beta z}$, and let $g(s) = f(\log(s)/\beta)$. Under this transformation, the region R is mapped to a closed simply connected region that lies in the half-plane $\mathrm{Re}(w) > 0$. Thus g/ψ_β^N is analytic in this region in the w-plane, and we can use the Hermite formula for the error in polynomial interpolation [5],

$$\begin{aligned} g(s) - G(s) &= \psi_\beta^N(s) \left(\frac{g(s)}{\psi_\beta^N(s)} - \sum_{k=0}^{N} \tilde{\lambda}_k s^k \right) \\ &= \frac{\psi_\beta^N(s) \prod_{k=0}^{N} (s - s_k)}{2\pi i} \int_{\mathcal{C}} \frac{g(w)}{(w-s)\psi_\beta^N(w) \prod_{k=0}^{N} (w - s_k)} dw, \end{aligned}$$

where $s_k = e^{\beta x_k}$ and $\mathcal{C}$ is the image of C in the w-plane. A change of variables completes the proof. ∎

We now turn our attention to necessary conditions for uniform convergence of the interpolation process. To this end, we need the concept of limiting node density functions. These functions describe how the density of node distributions varies over $[-1, 1]$ as $N \to \infty$ [10, 16]. Given a node density function μ, it follows that the node locations x_j satisfy [10]

$$\frac{j}{N} = \int_{-1}^{x_j} \mu(x) dx, \qquad j = 0, \ldots, N.$$

Since our analysis parallels the convergence proof for polynomial interpolation (see, e.g., [5, 16, 24]), define

$$u_\beta(z) = \frac{\beta}{4} \mathrm{Re}\left[(z+1)^2\right] - \int_{-1}^{1} \log(|e^{\beta z} - e^{\beta t}|) \mu(t) dt. \tag{2.3}$$

We shall refer to this function as the *logarithmic potential* and to its level curves as *equipotentials*.

In the theorem below we shall assume that μ is such that there exist a and b, $a < b$, with the property that if $K \in [a, b]$, then there exists a simple, closed, rectifiable curve that satisfies $u_\beta(z) = K$ and contains the interval $[-1, 1]$ in its interior. We denote this curve by C_K and by R_K the part of the plane which lies inside it. We also require that if $K_1 > K_2$, then $R_{K_1} \subset R_{K_2}$. To illustrate this feature, consider the logarithmic potential for uniformly distributed nodes on $[-1, 1]$ and $\beta = 1$. In this case we have that $\mu(t) = 1/2$. The level curves of u_1 are presented in Figure 2.1. In this instance one could choose $a = 0.5$ and $b = 0.7$.

THEOREM 2.2. *Suppose μ satisfies the properties above, and let B be the closure of R_b. If f is an analytic function in an open region R which lies inside the strip $-\pi/(2\beta) < \mathrm{Im}(z) < \pi/(2\beta)$ and contains B in its interior, then the GRBF interpolation described above converges uniformly with respect to $z \in B$.*

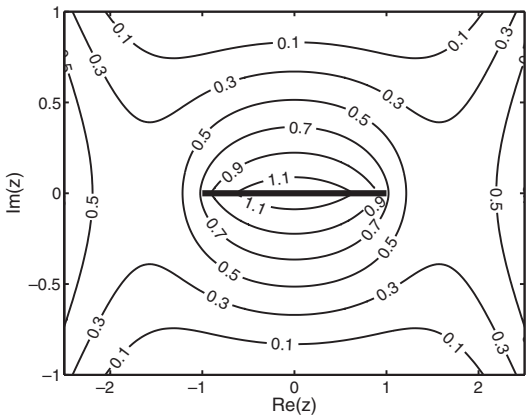

FIG. 2.1. *Level curves of the logarithmic potential for $\beta = 1$ and $\mu(t) = 1/2$. The straight line represents the interval $[-1, 1]$.*

Proof. Since R is open and B is closed, there exist K_1 and K_2 such that $K_1 < K_2 < b$ and $R_{K_1} \cup C_{K_1}$ lies inside R. Using Lemma 2.1, we have that for any x on C_{K_2},

$$|f(x) - F(x)| \leq \frac{\beta M}{2\pi\delta} \int_{C_{K_1}} \frac{|\eta_N(x)|}{|\eta_N(z)|} dz, \tag{2.4}$$

where M is the largest value of $|f(z)e^{\beta z}|$ on C_{K_1} and δ is the smallest value of $|e^{\beta z} - e^{\beta x}|$ for $z \in C_{K_1}$ and $x \in C_{K_2}$.

We also have that

$$\frac{|\eta_N(x)|}{|\eta_N(z)|} = \exp\left\{-N\left(\log|\eta_N(z)|^{\frac{1}{N}} - \log|\eta_N(x)|^{\frac{1}{N}}\right)\right\}. \tag{2.5}$$

A bound on this exponential can be obtained using the limiting logarithmic potential. Notice that

$$\lim_{N\to\infty} \log|\eta_N(z)|^{\frac{1}{N}} = -u_\beta(z) = -K_1 \quad \text{for } z \in C_{K_1}$$

and

$$\lim_{N\to\infty} \log|\eta_N(x)|^{\frac{1}{N}} = -u_\beta(x) = -K_2 \quad \text{for } x \in C_{K_2}.$$

Hence, for any given ϵ, $0 < \epsilon < (K_2 - K_1)/2$, there exists N_ϵ such that for $N > N_\epsilon$

$$\begin{aligned} -K_1 - \epsilon < \log|\eta_N(z)|^{\frac{1}{N}} < -K_1 + \epsilon, \\ -K_2 - \epsilon < \log|\eta_N(x)|^{\frac{1}{N}} < -K_2 + \epsilon, \end{aligned}$$

which implies that

$$\log|\eta_N(z)|^{\frac{1}{N}} - \log|\eta_N(x)|^{\frac{1}{N}} < m_\epsilon, \tag{2.6}$$

where $m_\epsilon = K_2 - K_1 + 2\epsilon > 0$.

Combining (2.4), (2.5), and (2.6) gives

$$|f(x) - F(x)| \leq \frac{\beta M \kappa}{2\pi\delta} e^{-N m_\epsilon}, \quad N > N_\epsilon,\ x \in C_{K_2}, \tag{2.7}$$

where κ is the length of C_{K_1}.

This last inequality implies that $|f - F| \to 0$ uniformly as $N \to \infty$ on C_{K_2}. Since $f - F$ is analytic in R_{K_2}, by the maximum modulus principle we have that F converges uniformly to f in R_{K_2}. ∎

We point out that, as happens in polynomial interpolation, the convergence in (2.7) is exponential with a rate that is governed by the equipotentials induced by the nodes.

2.1. The Runge phenomenon. The Runge phenomenon is well understood in polynomial interpolation in one dimension [5, 9] . Even if a function is smooth on the interpolation interval $[-1, 1]$, polynomial interpolants will not converge to it uniformly as $N \to \infty$ unless the function is analytic in a larger complex region whose shape depends on the interpolation nodes. Clustering nodes more densely near the ends of the interval avoids this difficulty. Specifically, points distributed with density $\pi^{-1}(1 - x^2)^{-1/2}$, such as Chebyshev extreme points $x_j = -\cos(j\pi/N)$ and zeros of Chebyshev and Legendre polynomials, are common choices of interpolation nodes on $[-1, 1]$. Uniform convergence of polynomial interpolants is guaranteed for these nodes as long as the function being interpolated is analytic inside an ellipse with foci ± 1 and semiminor larger than δ, for some $\delta > 0$ [9].

In this section we show that for GRBFs uniform convergence may be lost, not only in the polynomial limit $c \to \infty$ but also for constant β (which implies $c \to 0$ as $N \to \infty$), if the distribution of interpolation nodes is not chosen appropriately. Theorem 2.2 can be used to state the regularity requirements of the function being interpolated using a given node distribution, enabling us to determine whether the interpolation process is convergent.

We point out that, for $\beta \ll 1$,

$$u_\beta(z) = -\log(\beta) - \int_{-1}^{1} \log|z - t| \mu(t) dt + O(\beta). \tag{2.8}$$

In this case, the level curves of u_β are similar to equipotentials of polynomial interpolation, and the convergence of the GRBF interpolation process can be predicted from the well-known behavior of polynomial interpolation.

Equipotentials for $\beta = 0.1, 0.8, 2, 5$ are presented in Figure 2.2. On the left of this figure, we present contour maps obtained with a uniform node distribution, and on the right, contour maps obtained with the Chebyshev extreme points. Equipotentials for $\beta = 0.1$ are similar to equipotentials for polynomial interpolation [9], as expected. By Theorem 2.2, convergence is guaranteed if the function is analytic inside the contour line that surrounds the smallest equipotential domain that includes $[-1, 1]$, whereas any singularity inside this region leads to spurious oscillations that usually grow exponentially. Therefore, it is desirable to have the region where the function is required to be analytic be as small as possible. In this sense, we note that for $\beta = 0.1$ the Chebyshev distribution is close to optimal, and for $\beta = 5$ a uniform distribution seems to be more appropriate. We also note that, for large β, Chebyshev density overclusters the nodes near the ends of the interval. In fact, if this clustering is used with $\beta = 5$, even the interpolation of $f \equiv 1$ is unstable; in this case there is no equipotential region that encloses $[-1, 1]$.

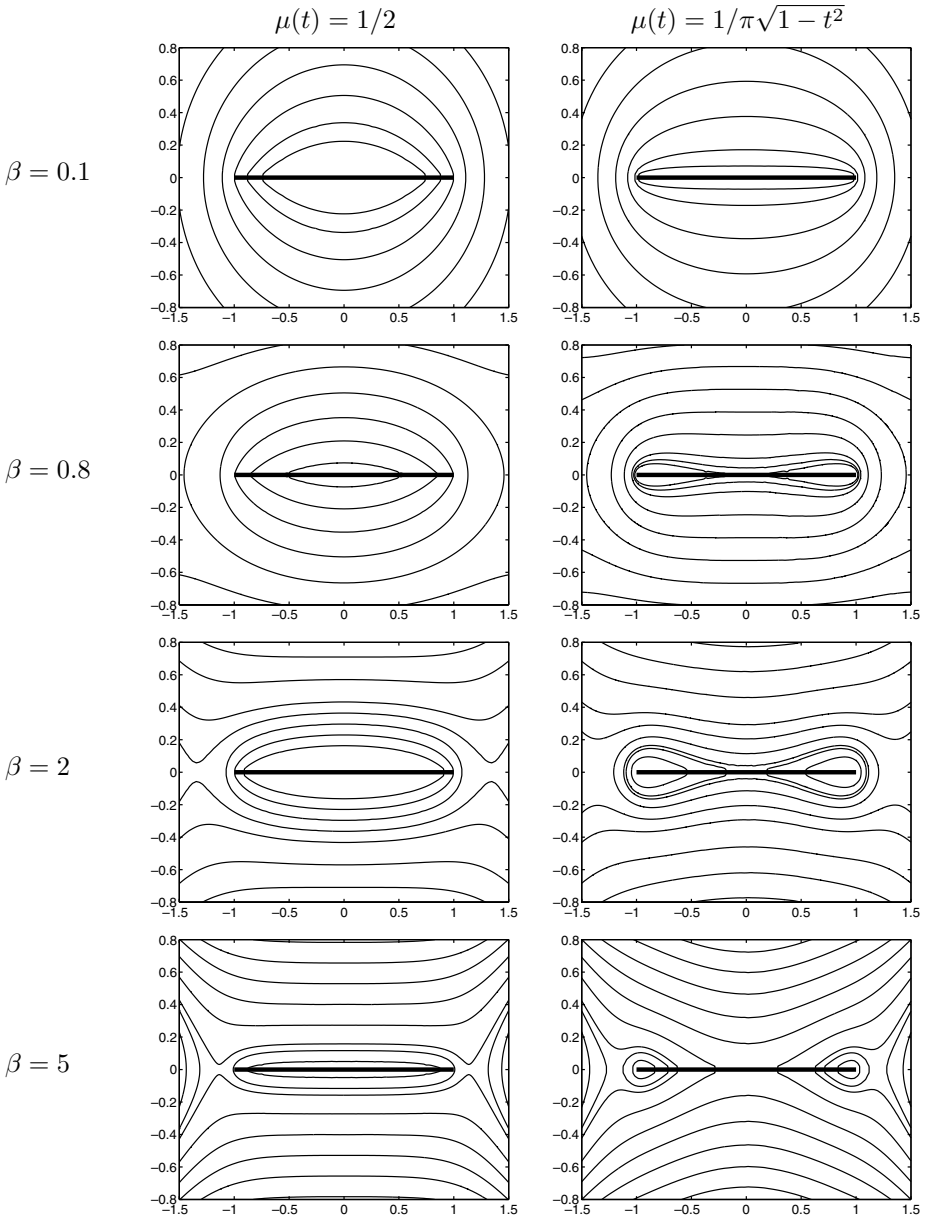

FIG. 2.2. *Contour maps of the logarithmic potential. Plots on the left were obtained with uniform node distribution. Plots on the right were obtained with Chebyshev distribution.*

To demonstrate how the equipotentials and singularities of the interpolated function restrict the convergence of GRBF interpolation, in Figures 2.3 and 2.4 we show two pairs of interpolants. Each pair consists of one function that leads to the Runge phenomenon and one that leads to a stable interpolation process. In Figure 2.3, equispaced nodes were used. The interpolation of $f(x) = 1/(4 + 25x^2)$ is convergent, while the interpolation of $f(x) = 1/(1 + 25x^2)$ is not. Notice from Figure 2.2 that the former function is singular at points inside the smallest equipotential domain,

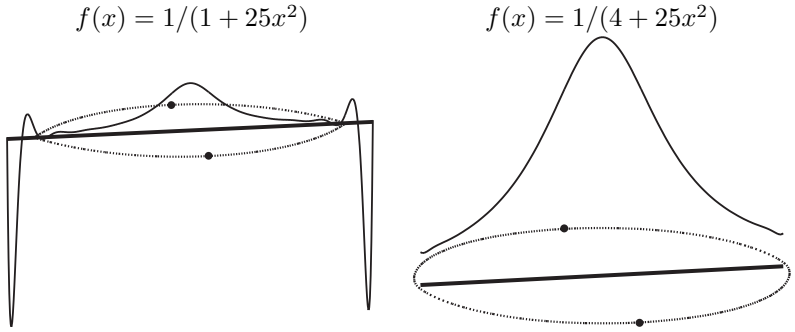

FIG. 2.3. *Interpolation of f with 25 equispaced nodes and $\beta = 0.8$. Closed curves are level curves of the logarithmic potential, dots mark the singularities of f, and straight lines represent the interval $[-1, 1]$.*

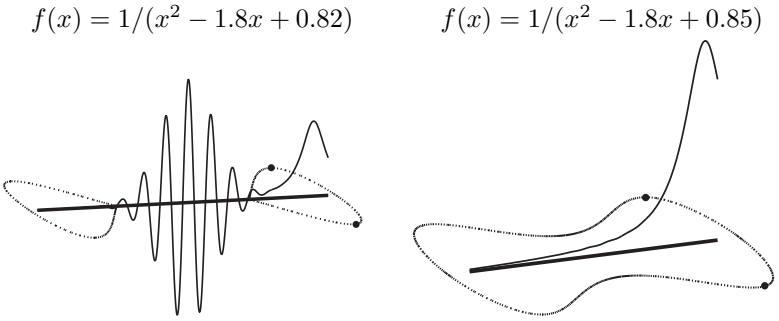

FIG. 2.4. *Interpolation of f with 41 Chebyshev nodes and $\beta = 2$. Closed curves are level curves of the logarithmic potential, dots mark the singularities of f, and straight lines represent the interval $[-1, 1]$.*

and the singularities of the latter function lie outside this region. For Chebyshev nodes and $\beta = 2$, interpolation of $f(x) = 1/(x^2 - 1.8x + 0.82)$ generates spurious oscillation in the center of the interval. Interpolation of a slightly different function, $f(x) = 1/(x^2 - 1.8x + 0.85)$, gives a well-behaved interpolant.

2.2. Lebesgue constants. Although Theorem 2.2 guarantees convergence for sufficiently smooth functions and properly chosen interpolation points, approximations may not converge in the presence of rounding errors due to the rapid growth of the Lebesgue constant. For GRBF interpolation, we define the Lebesgue constant by

$$\Lambda_N^{GRBF} = \max_{x\in[-1,1]} \sum_{k=0}^{N} |L_k(x)|, \tag{2.9}$$

where

$$L_k(x) = e^{-\frac{N\beta}{4}\left((x+1)^2-(x_k+1)^2\right)} \prod_{\substack{j=0 \\ j\neq k}}^{N} \frac{(e^{\beta x} - e^{\beta x_j})}{(e^{\beta x_k} - e^{\beta x_j})} \tag{2.10}$$

is the GRBF cardinal function. Notice that $L_k(x_k) = 1$, $L_k(x_j) = 0$ $(j \neq k)$, and by (2.2), $L_k(x) \in \text{Span}\{e^{-(x-\xi_k)^2/c^2}\}$. Thus, the unique GRBF interpolant can be

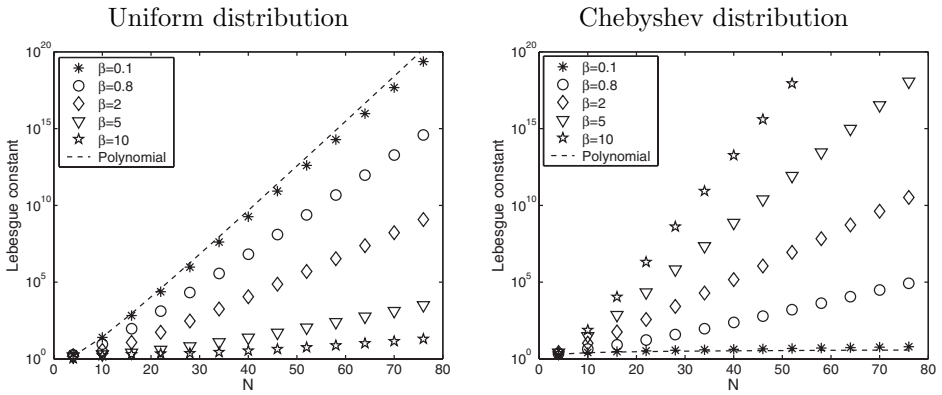

FIG. 2.5. *Lebesgue constant for different values of β. Dashed lines mark the Lebesgue constant values for polynomial interpolation.*

written as

$$F(x) = \sum_{k=0}^{N} L_k(x) f(x_k), \tag{2.11}$$

and it follows that

$$\|F - f\|_\infty \leq (1 + \Lambda_N^{GRBF}) \|F^{opt} - f\|_\infty, \tag{2.12}$$

where F^{opt} is the best approximation to f in the GRBF subspace with respect to the infinity norm.

Figure 2.5 illustrates how the GRBF Lebesgue constant grows with N for equispaced nodes (left) and Chebyshev nodes (right). As expected, for small β the GRBF Lebesgue constants approximate the polynomial Lebesgue constants, which behave asymptotically as $O(2^N/(N \log N))$ for equispaced nodes and $O(\log N)$ for Chebyshev nodes [9, 23]. This figure shows that the Lebesgue constants grow exponentially for both node distributions, except for large values of β for uniform nodes and small values of β for Chebyshev nodes.

In the presence of rounding errors, (2.12) indicates that if computations are carried out with precision ε, then the solution will generally be contaminated by errors of size $\varepsilon \Lambda_N^{GRBF}$ [23]. For instance, if $f(x) = 1/(x^2 - 1.8x + 0.85)$ and $\beta = 2$, the convergence of the interpolation process on Chebyshev nodes in double precision stops at $N = 80$, with a minimum residue of $O(10^{-7})$ due to rounding error. Similar results have been observed on equispaced nodes if β is small.

2.3. Stable interpolation nodes. Our goal now is to find node distributions that lead to a convergent interpolation process whenever the function is analytic on $[-1, 1]$. This happens only if $[-1, 1]$ is itself an equipotential, as is the case for Chebyshev density in polynomial interpolation. Therefore, we seek a density function μ that satisfies

$$\frac{\beta}{4}(x+1)^2 = \int_{-1}^{1} \log(|e^{\beta x} - e^{\beta t}|)\mu(t)dt \ + \ \text{constant}, \quad x \in [-1, 1]. \tag{2.13}$$

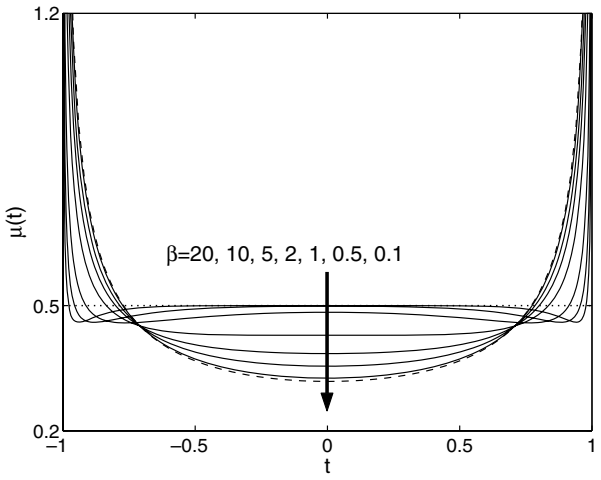

FIG. 2.6. *Numerical approximations of the optimal density functions for several values of β. The dashed line shows the Chebyshev density function.*

In order to find a numerical solution to this integral equation, we assume that the optimal μ can be approximated by

$$\mu(t) \cong \sum_{k=0}^{N_\mu} a_k \frac{T_{2k}(t)}{\sqrt{1-t^2}}, \tag{2.14}$$

where T_{2k} is the Chebyshev polynomial of order $2k$. We consider only even functions in our expansion because we expect the density function to be even due to symmetry. This generalizes the Chebyshev density function $\mu(t) = \pi^{-1}(1-t^2)^{-1/2}$. We also tried more general expressions, replacing $\sqrt{1-t^2}$ with $(1-t^2)^{-\alpha}$, and found that $\alpha = 1/2$ was suitable.

Figure 2.6 shows density functions computed with the expression above. We computed the coefficients a_k by discrete least-squares, and the integral in (2.13) was approximated by Gaussian quadrature. We used $N_\mu = 9$ and 50 points to evaluate the residue in the least-squares process. With this choice of parameters, the residual was less than 10^{-7} in all computations.

In Figure 2.7 we show 21 nodes computed using (2.13) and (2.14) for several values of β. For large values of β the nodes are nearly equally spaced, and for small values they are approximately equal to Chebyshev extreme points. The optimal equipotentials obtained for $\beta = 0.1, 0.8, 2, 5$ are presented in Figure 2.8. For all these values of β, $[-1, 1]$ seems to be a level curve of the logarithmic potential.

As mentioned in section 2.2, in the presence of rounding errors the Lebesgue constant also plays a crucial role. Fortunately, for the optimal nodes computed numerically in this section, experiments suggest that the Lebesgue constant grows at a logarithmic rate. Figure 2.9 presents computed Lebesgue constants for different values of β on optimal nodes.

Figure 2.10 shows the convergence of the GRBF interpolation to the four functions used to illustrate the Runge phenomenon in section 2.1. Now all four functions can be approximated nearly to machine precision. The algorithm used to obtain these

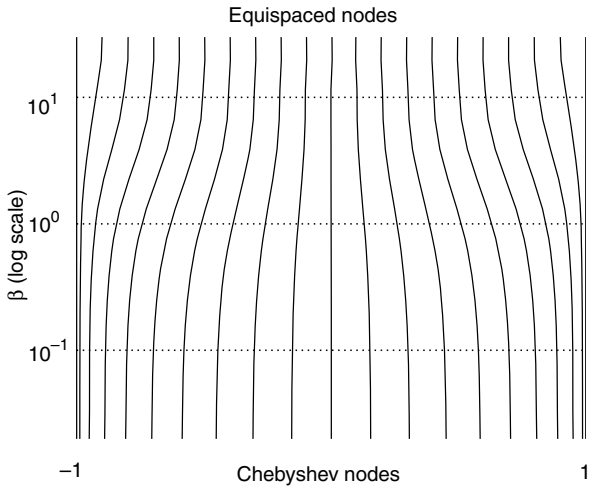

FIG. 2.7. *Node locations obtained using a density function computed by solving the integral equation* (2.13) *for* $N = 20$ *and several values of* β.

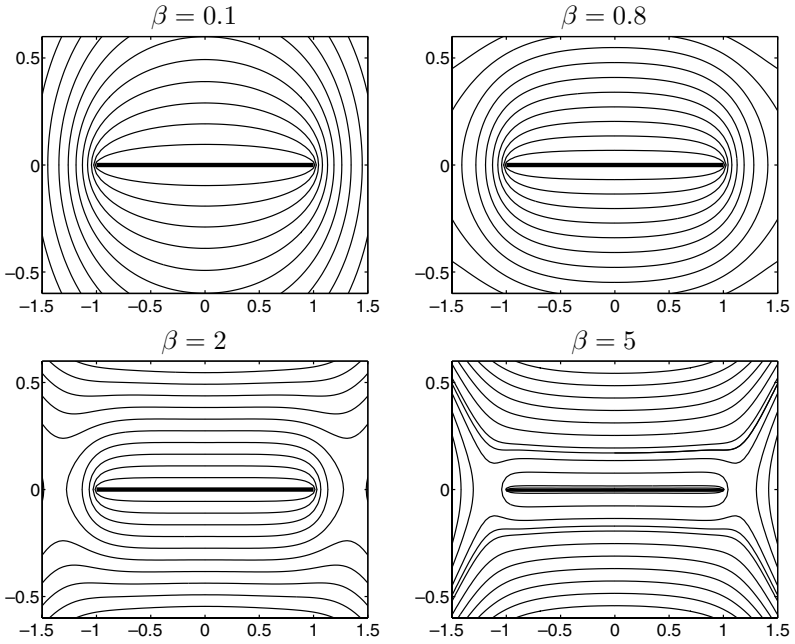

FIG. 2.8. *Contour maps of the logarithmic potential obtained with a numerically approximated optimal density function.*

data is presented in section 3. Notice that the convergence rates are determined by the singularities of the function being interpolated. Dashed lines in this figure mark the convergence rates predicted by (2.7). For instance, if $f(x) = 1/(1 + 25x^2)$ and $\beta = 0.8$, then m_ϵ is approximately the difference between the value of the potential in $[-1, 1]$ and the potential at $z = 0.2i$ (where f is singular), giving $m_\epsilon \cong 0.23$.

Notice that for $\beta = 2$ the equipotentials that enclose the interval $[-1, 1]$ are

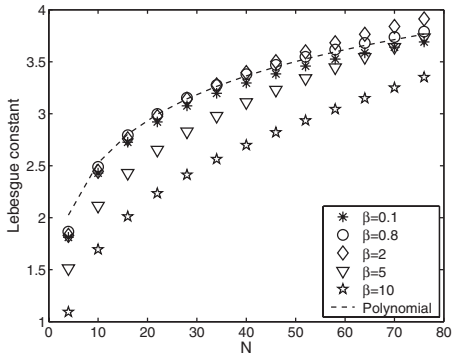

FIG. 2.9. *Lebesgue constant for different values of β and optimal node distribution.*

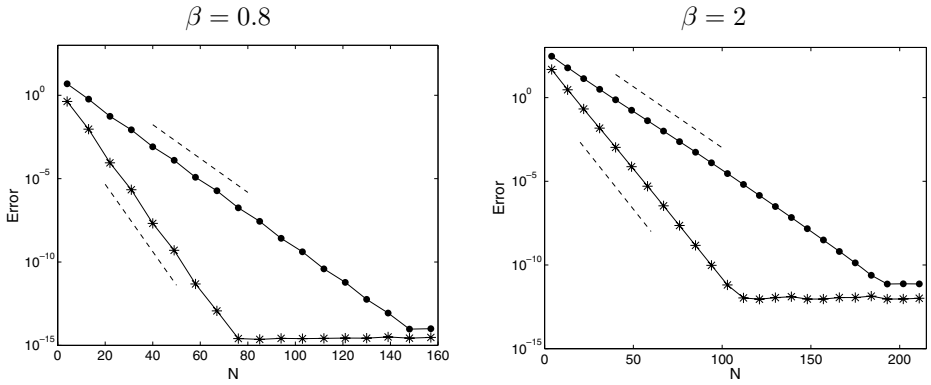

FIG. 2.10. *Maximum error of the interpolation process using optimal nodes. Left:* $f(x) = 1/(1+25x^2)$ *(•) and* $f(x) = 1/(4+25x^2)$ *(∗). Right:* $f(x) = 1/(x^2 - 1.8x + 0.82)$ *(•) and* $f(x) = 1/(x^2 - 1.8x + 0.85)$ *(∗). Dashed lines mark convergence rates predicted by* (2.7).

contained in a bounded region (Figure 2.8). This indicates that the convergence rate given by (2.7) is the same for *all* functions that have singularities outside this region. In polynomial interpolation, convergence to entire functions is much faster than to functions with finite singularities. This is not the case for GRBFs. With $\beta = 2$ we found that the rate of convergence of interpolants of $1/(1+4x^2)$, $1/(100+x^2)$, $\sin(x)$, and $|x+2|$ were all about the same. What these functions have in common is that they are analytic inside the smallest region that includes all equipotentials that enclose $[-1, 1]$.

It is also worth noting that the one-parameter family μ_γ of node density functions proportional to $(1-t^2)^{-\gamma}$ [9] was used in [10] and [20] to cluster nodes near boundaries in RBF approximations. Although numerical results there showed improvement in accuracy, no clear criteria for choosing γ was provided in those papers. By using these node density functions and minimizing the residue in (2.13) with respect to γ, we found that optimal values of γ are approximately given by $\gamma \cong 0.5e^{-0.3\beta}$. We point out, however, that interpolations using these density functions may not converge if large values of N are required.

2.4. Location of centers. Up to this point we have assumed that the centers are uniformly distributed on $[-1, 1]$. Here we briefly investigate the consequences of

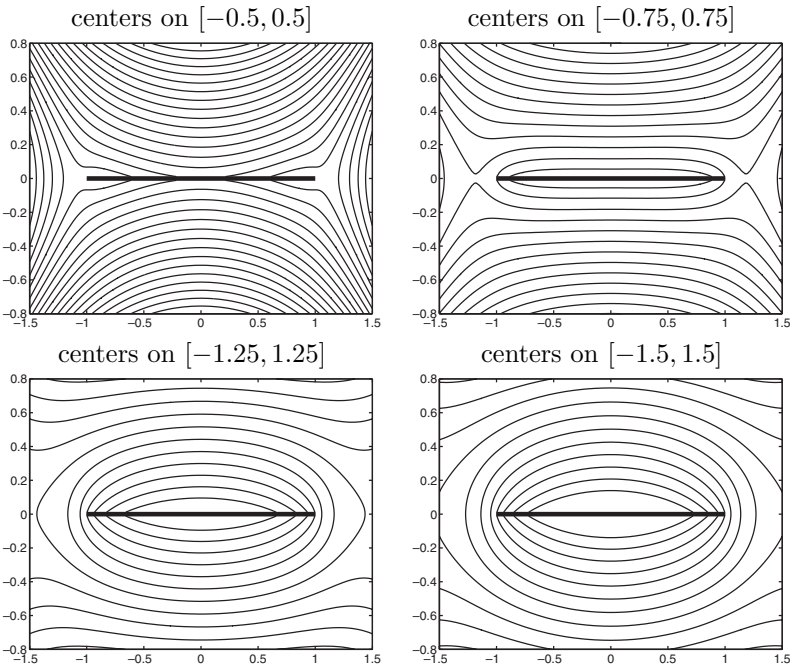

FIG. 2.11. *Equipotentials for $\beta = 2$ (compare with Figure 2.2). Uniformly distributed centers on interval specified above. Interpolation points are uniformly distributed on* $[-1, 1]$.

choosing centers ξ_k that are equispaced on the interval $[-L, L]$, where $L \neq 1$, and also discuss results where centers are not equally spaced. Taking centers outside the interval of approximation, as was suggested in [10, 17] to improve edge accuracy, is of practical interest.

For equispaced centers on $[-L, L]$, a straightforward modification of (2.2) gives

$$F(x) = e^{\frac{-N\beta}{4L}(x+L)^2} \sum_{k=0}^{N} \tilde{\lambda}_k e^{k\beta x},$$

where $\beta = 4L/Nc^2$. In this case the logarithmic potential becomes

$$u_\beta^L(z) = \frac{\beta}{4L} \operatorname{Re}\left[(z+L)^2\right] - \int_{-1}^{1} \log(|e^{\beta z} - e^{\beta t}|)\mu(t)dt.$$

Equipotentials for different values of L are presented in Figure 2.11. We considered equispaced interpolation nodes on $[-1, 1]$. Notice that if $L = 0.5$, there is no guarantee of convergence, as no equipotential encloses $[-1, 1]$. For L =0.75, 1.25, and 1.5, there are equipotentials enclosing this interval. The region where f is required to be smooth seems to increase with L. We also point out that the asymptotic behavior for small β, given in (2.8), holds independently of L, indicating that center location is irrelevant in the polynomial limit.

It is common practice to choose the same nodes for centers and interpolation. In Figure 2.12 we show the graphs of the GRBF interpolants, for $f(x) = 1/(x^2 - 1.8x + 0.82)$ and $f(x) = 1/(x^2 - 1.8x + 0.85)$, where both centers and interpolation nodes are Chebyshev points. These data suggest that interpolation with Chebyshev centers also

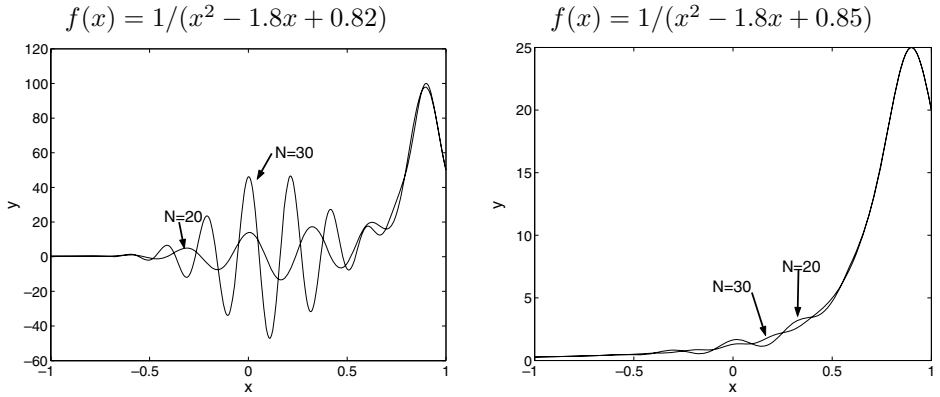

FIG. 2.12. *GRBF interpolation using Chebyshev points for centers and interpolation nodes,* $\beta = 2$.

suffers from the Runge phenomenon. These results are similar to the ones obtained in Figure 2.4 for equispaced centers. Notice that we cannot use the definition involving h for β if the centers are not equispaced; in this case we use the definition $\beta = 4/(Nc^2)$.

3. Algorithmic implications. It is well known that most RBF-based algorithms suffer from ill-conditioning. The interpolation matrix $[\phi(\|x_i - \xi_j\|)]$ in most conditions becomes ill-conditioned as the approximations get more accurate, to the extent that global interpolants are rarely computed for more than a couple of hundred nodes. Based on numerical and theoretical observations, in [22] Schaback states that for RBFs, "Either one goes for a small error and gets a bad sensitivity, or one wants a stable algorithm and has to take a comparably larger error." Several researchers have addressed this issue [4, 8, 15, 21]. In particular, Fornberg and Wright [12] recently presented a contour-integral approach that allows numerically stable computations of RBF interpolants for all values of the free parameter c, but this technique is expensive and has been applied only for experimental purposes.

For GRBFs with equispaced centers, (2.11) provides an explicit interpolation formula through the use of the cardinal functions L_k, so the difficulty of inverting the interpolation matrix can be avoided. This is equivalent to Lagrange polynomial interpolation.

Notice that the exponential term $e^{-\frac{N\beta}{4}((x+1)^2-(x_k+1)^2)}$ in (2.10) becomes very close to zero for certain values of x if N is large, affecting the accuracy of the approximations. A simple modification of (2.10) improves matters:

$$L_k(x) = \prod_{\substack{j=0 \\ j\neq k}}^{N} \frac{e^{-\frac{\beta}{4}\left((x+1)^2-(x_k+1)^2\right)}\left(e^{\beta x} - e^{\beta x_j}\right)}{\left(e^{\beta x_k} - e^{\beta x_j}\right)}. \tag{3.1}$$

The direct implementation of (3.1) together with (2.11) provides a simple algorithm for computing the GRBF interpolant for moderate values of N. In our experiments, effective computations were carried out up to $N = 300$. We shall next derive a more stable formula to handle larger problems.

In [1] Berrut and Trefethen point out the difficulties of using the standard Lagrange formula for practical computations and argue that the barycentric form of Lagrange interpolation should be the method of choice for polynomial interpolation.

For GRBFs we define the barycentric weights by

$$w_k = \left(\prod_{\substack{j=0 \\ j\neq k}}^{N} e^{-\frac{\beta}{4}(x_k+1)^2} \left(e^{\beta x_k} - e^{\beta x_j} \right) \right)^{-1}, \tag{3.2}$$

and thus we have that

$$L_k(x) = L(x) \frac{w_k}{e^{-\frac{\beta}{4}(x+1)^2} \left(e^{\beta x} - e^{\beta x_k} \right)} \qquad (x \neq x_k),$$

where

$$L(x) = \prod_{j=0}^{N} e^{-\frac{\beta}{4}(x+1)^2} \left(e^{\beta x} - e^{\beta x_j} \right).$$

Therefore, the GRBF interpolant can be written as

$$F(x) = L(x) \sum_{k=0}^{N} \frac{w_k}{e^{-\frac{\beta}{4}(x+1)^2} \left(e^{\beta x} - e^{\beta x_k} \right)} f(x_k). \tag{3.3}$$

For reasons of numerical stability, it is desirable to write L as a sum involving the barycentric weights. For polynomial interpolation this is done by considering that 1 can be exactly written in terms of interpolation formulas, since it is itself a polynomial. Unfortunately, a constant function is not exactly represented in terms of GRBFs. Nevertheless, this difficulty can be circumvented if we properly choose a function that belongs to the GRBF space. In our implementation, we consider the function

$$v(x) = \frac{1}{N} \sum_{k=0}^{N} e^{-\frac{N\beta}{4}(x-\xi_k)^2}.$$

Notice that in this case,

$$L(x) = \frac{v(x)}{\sum_{k=0}^{N} \frac{w_k}{e^{-\frac{\beta}{4}(x+1)^2} \left(e^{\beta x} - e^{\beta x_k} \right)} v(x_k)}.$$

Combining the last expression with (3.3) gives our *GRBF barycentric formula*:

$$F(x) = v(x) \frac{\sum_{k=0}^{N} \frac{w_k}{\left(e^{\beta x} - e^{\beta x_k} \right)} f(x_k)}{\sum_{k=0}^{N} \frac{w_k}{\left(e^{\beta x} - e^{\beta x_k} \right)} v(x_k)}. \tag{3.4}$$

As mentioned in [1], the fact that the weights w_k appear symmetrically in the denominator and in the numerator means that any common factor in all the weights may be canceled without affecting the value of F. In some cases it is necessary to rescale terms in (3.2) to avoid overflow. In our implementation we divided each term by $\prod_{j=1}^{N} |e^{\beta x_j} - e^{-\beta}|^{1/N}$.

In [13] Higham shows that for polynomials the barycentric formula is forward stable for any set of interpolation points with a small Lebesgue constant. Our numerical experiments suggest that the GRBF barycentric formula is also stable.

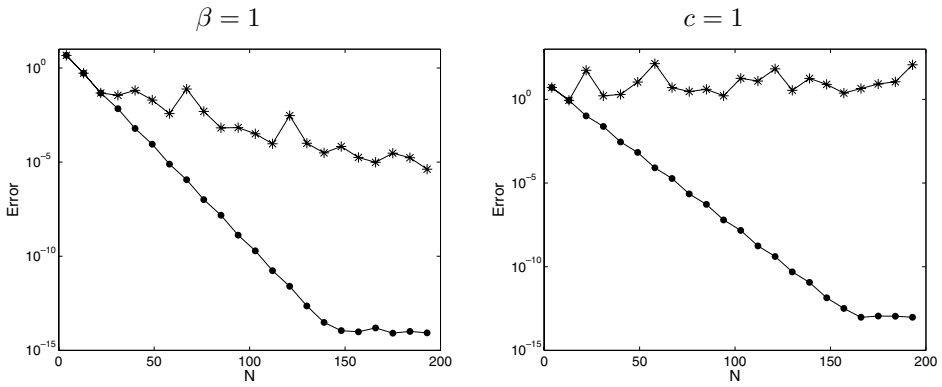

FIG. 3.1. *Maximum error of the interpolation of* $f(x) = 1/(1 + 25x^2)$ *using barycentric interpolation* (•) *and the standard RBF algorithm* (∗). *Left:* β *fixed. Right:* c *fixed.*

Figure 2.10 was obtained using the barycentric formula. We point out that the direct inversion of the interpolation matrix becomes unstable even for moderate values of N. In Figure 3.1 we compare the convergence of the GRBF interpolant computed with the barycentric formula with that found by inverting the interpolation matrix (standard RBF algorithm). We first computed approximations with β fixed (left graph). Notice that for the standard implementation, convergence rate changes at a level around 10^{-2}, and the method becomes very inefficient for larger values of N. For the barycentric formula, on the other hand, convergence continues to machine precision. For these approximations we used nodes computed with an approximate optimal density function, as in section 2.3.

We also compared the algorithms for fixed c (right graph). In this instance we used Chebyshev nodes, as c constant implies that $\beta \to 0$ as N becomes large and approximations become polynomial. The performance of the standard algorithm is even worse in this case.

4. Final remarks. GRBFs using equally spaced centers are easily related to polynomials in a transformed variable through (2.2). This connection allows us to apply polynomial interpolation and potential theory to draw a number of precise conclusions about the convergence of GRBF interpolation. In particular, for a given interpolation node density, one can derive spectral convergence (or divergence) rates based on the singularity locations of the target function. Conversely, one can easily compute node densities for which analyticity of the function in $[-1, 1]$ is sufficient for convergence and for which the Lebesgue constant is controlled. Furthermore, the polynomial connection allows us to exploit barycentric Lagrange interpolation to construct a simple explicit interpolation algorithm that avoids the ill-conditioning of the interpolation matrix. We stress that the convergence illustrated in Figure 3.1 is made possible only through the use of *both* the stable nodes and the stable algorithm.

Numerical evidence suggests that other RBFs such as multiquadrics may also be susceptible to the Runge phenomenon and dependent on node location for numerically stable interpolations. Figure 4.1 shows graphs of multiquadric interpolants of two functions. We first considered the small β case (nearly polynomial) with the same function that caused the Runge phenomenon for GRBFs on equispaced nodes. The high oscillations of the interpolant at the ends of the interval indicates that this function also causes the Runge phenomenon for multiquadrics. The multiquadric

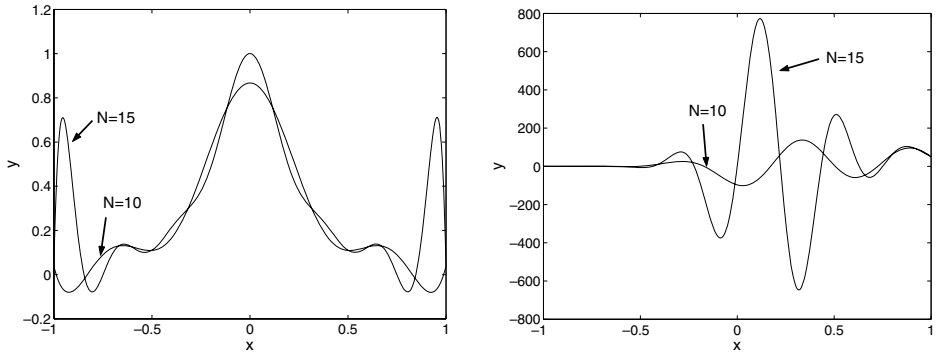

FIG. 4.1. *Runge phenomenon in multiquadric RBF interpolation. Left: Interpolation of* $f(x) = 1/(1+25x^2)$ *using equispaced nodes and* $\beta = 0.1$. *Right: Interpolation of* $f(x) = 1/(x^2 - 1.8x + 0.82)$ *using Chebyshev nodes and* $\beta = 2$.

interpolant of $f(x) = 1/(x^2 - 1.8x + 0.82)$ with $\beta = 2$ and equispaced centers also presented spurious oscillations, as its GRBF counterpart did, when Chebyshev interpolation nodes were used.

Practical interest in RBF methods is fueled by their flexibility in the node and center locations and by their simple use in higher-dimensional approximation. The results of this paper do not extend immediately in either of those directions, except to a tensor-product situation of uniform center locations in a box. Still, we believe that the explicit GRBF interpolation algorithm, in particular, may be adaptable to selective resolution requirements and geometric flexibility.

REFERENCES

[1] J.-P. BERRUT AND L. N. TREFETHEN, *Barycentric Lagrange interpolation*, SIAM Rev., 46 (2004), pp. 501–517.
[2] M. BOZZINI, L. LENARDUZZI, AND R. SCHABACK, *Adaptive interpolation by scaled multiquadrics*, Adv. Comput. Math., 16 (2002), pp. 375–387.
[3] M. D. BUHMANN, *Radial Basis Functions*, Cambridge University Press, Cambridge, UK, 2003.
[4] A. H.-D CHENG, M. A. GOLBERG, E. J. KANSA, AND G. ZAMMITO, *Exponential convergence and H-c multiquadric collocation method for partial differential equations*, Numer. Methods Partial Differential Equations, 19 (2003), pp. 571–594.
[5] P. J. DAVIS, *Interpolation and Approximation*, Dover, New York, 1975.
[6] T. A. DRISCOLL AND B. FORNBERG, *Interpolation in the limit of increasingly flat radial basis functions*, Comput. Math. Appl., 43 (2002), pp. 413–422.
[7] G. E. FASSHAUER, *Solving partial differential equations by collocation with radial basis functions*, in Surface Fitting and Multiresolution Methods, A. LeMéhauté, C. Rabut, and L. Schumaker, eds, Vanderbilt University Press, Nashville, TN, 1997, pp. 131–138.
[8] G. E. FASSHAUER, *Solving differential equations with radial basis functions: Multilevel methods and smoothing*, Adv. Comput. Math., 11 (1999), pp. 139–159.
[9] B. FORNBERG, *A Practical Guide to Pseudospectral Methods*, Cambridge University Press, New York, 1996.
[10] B. FORNBERG, T. A. DRISCOLL, G. WRIGHT, AND R. CHARLES, *Observations on the behavior of radial basis function approximations near boundaries*, Comput. Math. Appl., 43 (2002), pp. 473–490.
[11] B. FORNBERG AND N. FLYER, *Accuracy of radial basis function interpolation and derivative approximations on* 1*-D infinite grids*, Adv. Comput. Math., 23 (2005), pp. 5–20.
[12] B. FORNBERG AND G. WRIGHT, *Stable computation of multiquadric interpolants for all values of the shape parameter*, Comput. Math. Appl., 47 (2004), pp. 497–523.

[13] N. J. Higham, *The numerical stability of barycentric Lagrange interpolation*, IMA J. Numer. Anal., 24 (2004), pp. 547–556.
[14] E. J. Kansa, *Multiquadrics—A scattered data approximation scheme with applications to computational fluid dynamics* II. *Solutions to hyperbolic, parabolic, and elliptic partial differential equations*, Comput. Math. Appl., 19 (1990), pp. 147–161.
[15] E. J. Kansa and Y. C. Hon, *Circumventing the ill-conditioning problem with multiquadric radial basis functions: Applications to elliptic partial differential equations*, Comput. Math. Appl., 39 (2000), pp. 123–137.
[16] V. I. Krylov, *Approximate Calculation of Integrals*, A. H. Stroud, trans., Macmillan, New York, 1962.
[17] E. Larsson and B. Fornberg, *A numerical study of some radial basis function based solution methods for elliptic PDEs*, Comput. Math. Appl., 46 (2003), pp. 891–902.
[18] W. R. Madych, *Miscellaneous error bounds for multiquadric and related interpolators*, Comput. Math. Appl., 24 (1992), pp. 121–138.
[19] W. R. Madych and S. A. Nelson, *Bounds on multivariate polynomials and exponential error estimates for multiquadric interpolation*, J. Approx. Theory, 70 (1992), pp. 94–114.
[20] R. B. Platte and T. A. Driscoll, *Computing eigenmodes of elliptic operators using radial basis functions*, Comput. Math. Appl., 48 (2004), pp. 561–576.
[21] S. Rippa, *An algorithm for selecting a good value for the parameter c in radial basis function interpolation*, Adv. Comput. Math., 11 (1999), pp. 193–210.
[22] R. Schaback, *Error estimates and condition numbers for radial basis function interpolation*, Adv. Comput. Math., 3 (1995), pp. 251–264.
[23] L. N. Trefethen and J. A. C. Weideman, *Two results on polynomial interpolation in equally spaced points*, J. Approx. Theory, 65 (1991), pp. 247–260.
[24] J. A. C. Weideman and L. N. Trefethen, *The eigenvalues of second-order spectral differentiation matrices*, SIAM J. Numer. Anal., 25 (1988), pp. 1279–1298.
[25] H. Wendland, *Gaussian interpolation revisited*, in Trends in Approximation Theory, K. Kopotun, T. Lyche, and N. Neamtu, eds., Vanderbilt University Press, Nashville, TN, 2001, pp. 1–10.
[26] J. Yoon, *Spectral approximation orders of radial basis function interpolation on the Sobolev space*, SIAM J. Math. Anal., 33 (2001), pp. 946–958.